Preprints of the 19th World Congress
The International Federation of Automatic Control
Cape Town, South Africa. August 24-29, 2014

Feedback Linearization-Based Control Approach for Air System of a Turbocharged SI Engine: Toward a Fuel-Optimal Strategy

AnhTu Nguyen, Michel Dambrine, Jimmy Lauber

LAMIH, UMR CNRS 8201, University of Valenciennes, France
E-mail: nguyen.trananhtu@gmail.com, {michel.dambrine, jimmy.lauber}@univ-valenciennes.fr

Michio Sugeno

European Center for Soft Computing
E-mail: michio.sugeno@gmail.com

Abstract: Combining turbocharging with downsizing has now become a key technique for automotive engine to improve its performance as fuel economy and drivability. The technology potential is fully exploited only with an efficient air path management system. In this context, the present work addresses a novel control design based on feedback linearization for the turbocharged air system of a SI engine. Two control strategies have been investigated for this complex system: drivability optimization and fuel reduction. The effectiveness of the proposed approach is evaluated via an advanced engine simulator.

Keywords: Turbocharged SI engine, feedback linearization, MIMO approach, fuel-optimal strategy.

1. Introduction

The air system control issue of turbocharged engine is known as a very interesting problem in automotive industry. Over the years, many control approaches have been proposed in the literature. However, up to now, it is still an active research subject in industry. The difficulties when dealing with this system are mainly due to the following facts. First, this MIMO system has a complex dynamics with several involved nonlinearities. Second, it is not easy to take into account the *fuel-optimal strategy* [1] in the control design when considering the whole system.

In the literature, most of works propose a decentralized control approach, i.e. one controller for each air actuator. In addition, linearization around operating points is often needed [2,3]. These controllers have some unavoidable drawbacks due to the application of linear control techniques to nonlinear systems. First, the tradeoff between performance and robustness throughout the wide engine operating range is difficult to achieve. Second, the calibration effort is very expensive. In [4], the authors proposed an interesting nonlinear approach for controlling the turbocharger of a SI engine which may significantly reduce the calibration task. However, this SISO approach allows only the wastegate control of the turbocharged engine air system. In addition, it needs some costly model simplification task. In [5], we have proposed a novel control strategy based on a switching Takagi-Sugeno model [6] which can get rid of the aforementioned difficulties. Although this powerful nonlinear controller provides satisfying closed-loop performance, it may look complex from an industrial point of view. In this paper, a second approach based on feedback linearization for the turbocharged air system which is much simpler (in the sense of control design and implementation) and can achieve practically a similar level of performance as the previous one. To the best of our knowledge, this is the second nonlinear MIMO controller that can guarantee the stability of the whole closed-loop turbocharged air system while taking into account the *fuel-optimal strategy* after [5,7] and the first nonlinear controller which is directly based on the complete nonlinear model of this system. Furthermore, the control approach proposed in this work could also limit the costly automotive sensors and/or observers/estimators design tasks by estimating all variables needed for control design by their static look-up-tables issued from the data of the test bench. Despite its simplicity, the simulation results carried out on an advanced simulator clearly show the effectiveness of the proposed control approach.

The paper is organized as follows. Section 2 presents a brief description on the air system of a turbocharged SI engine. Some bases on feedback linearization technique are recalled in Section 3. Section 4 is devoted to nonlinear control design and shows how to derive the *Fuel-optimal controller* from the proposed MIMO controller. Some simulation results are reported in Section 5. Finally, a concluding remark is provided in Section 6.

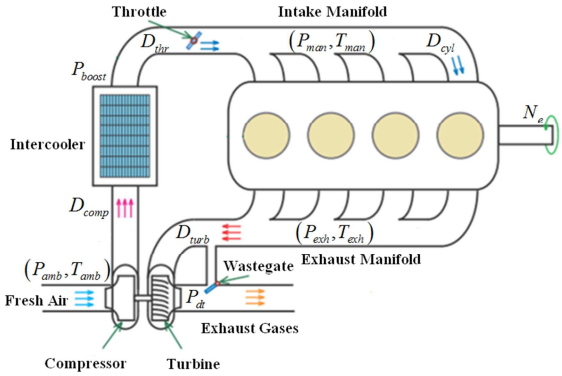

Figure 1. Schematic of a turbocharged SI engine

2. Turbocharged SI Engine Air System: a Brief Description

The studied air system is depicted in Figure 1. Hereafter, some main equations governing its behavior are recalled, please refer to [8,9] for more details.

The following notations will be used in this paper:

Variables	Description	Unit
P_{boost}	Boost pressure	Pa
P_{man}	Intake pressure	Pa
P_{exh}	Exhaust pressure	Pa
P_{amb}	Atmospheric pressure	Pa
$\Pi_{thr} \triangleq P_{man}/P_{boost}$	Throttle pressure ratio	--
$\Pi_{wg} \triangleq P_{dt}/P_{exh}$	Wastegate pressure ratio	--
$\Pi_{comp} \triangleq P_{boost}/P_{amb}$	Compressor pressure ratio	--
$\Pi_{turb} \triangleq P_{dt}/P_{exh}$	Turbine pressure ratio	--
T_{amb}	Atmospheric temperature	°K
T_{man}	Intake manifold temperature	°K
T_{exh}	Exhaust manifold temperature	°K
D_{thr}	Throttle mass air flow	kg/s
D_{wg}	Wastegate mass air flow	kg/s
D_{comp}	Compressor mass air flow	kg/s
D_{turb}	Turbine mass air flow	kg/s
D_{cyl}	Cylinder mass air flow	kg/s
D_{fuel}	Fuel injected flow	kg/s
V_{exh}	Exhaust manifold volume	m^3
V_{man}	Intake manifold volume	m^3
V_{cyl}	Cylinder volume	m^3
N_e	Engine speed	rpm
$\mathbb{P}_{comp}$	Compressor power	W
$\mathbb{P}_{turb}$	Turbine power	W
η_{comp}	Compressor isentropic efficiency	--
η_{turb}	Turbine isentropic efficiency	--
η_{vol}	Engine volumetric efficiency	--
λ_s	Stoichiometric air/fuel ratio	--
γ	Isentropic coefficient	--
R	Ideal gas constant	J/kg/°K
C_p	Specific heats at constant pressure	J/kg/°K

2.1. Intake and Exhaust Pressure Dynamics

Here, it is assumed that the volumes of the intake and exhaust manifolds are fixed, and that their thermodynamic conditions are homogeneous. In addition, the temperature dynamics are supposed to be negligible. Then, the isothermal filling-emptying model [8] is used to derive the intake and exhaust pressure dynamics:

$$\dot{P}_{man} = \frac{RT_{man}}{V_{man}}\left(D_{thr} - D_{cyl}\right) \tag{1}$$

$$\dot{P}_{exh} = \frac{RT_{exh}}{V_{exh}}\left(D_{cyl} + D_{fuel} - D_{turb} - D_{wg}\right) \tag{2}$$

Next, the mass air flow calculations will be detailed.

2.2. Air Flows Calculations

The actuator valves are modeled with the standard equations of compressible gas flow through a nozzle [9]:

$$D_{thr} = \Phi\left(\Pi^*_{thr}\right)\frac{P_{boost}}{\sqrt{RT_{man}}}u_{thr}; \quad D_{wg} = \Phi\left(\Pi^*_{wg}\right)\frac{P_{exh}}{\sqrt{RT_{exh}}}u_{wg} \tag{3}$$

where $\Phi(\Pi) \triangleq \sqrt{\frac{2\gamma}{\gamma-1}\left(\Pi^{2/\gamma} - \Pi^{(\gamma+1)/\gamma}\right)}$, $\Pi^*_{thr} \triangleq \max\left(\Pi_{thr}, \phi\right)$, $\Pi^*_{wg} \triangleq \max\left(\Pi_{wg}, \phi\right)$ and $\phi \triangleq \left(\frac{2}{\gamma+1}\right)^{\frac{\gamma}{\gamma-1}}$.

In (3), the two control inputs $u_{thr} \triangleq S_{thr}$ and $u_{wg} \triangleq S_{wg}$ are respectively the effective actuator opening sections of the throttle and of the wastegate. The in-cylinder air flow in (1) is computed as [8]:

$$D_{cyl} = \eta_{vol}\frac{P_{man}V_{cyl}}{RT_{man}}\frac{N_e}{30} \tag{4}$$

where $\eta_{vol} = \mathrm{LUT}_{\eta_{vol}}\left(N_e, P_{man}\right)$ is given by a look-up-table (LUT). Assume that the SI engine operates at stoichiometry; the fuel injected flow can be then deduced as follows:

$$D_{fuel} = \frac{1}{\lambda_s}D_{cyl} \tag{5}$$

2.3. Turbocharger Modeling

The turbocharger dynamics is modeled as:

$$\frac{d}{dt}\left(\frac{1}{2}J_{tc}N_{tc}^2\right) = \mathbb{P}_{turb} - \mathbb{P}_{comp} \tag{6}$$

where J_{tc} is the inertia of the turbocharger. The power consumed by the compressor is:

$$\mathbb{P}_{comp} = D_{comp}C_pT_{amb}\frac{1}{\eta_{comp}}\left(\Pi_{comp}^{\frac{\gamma-1}{\gamma}} - 1\right) \tag{7}$$

where the quantities $\Pi_{comp} = \mathrm{LUT}_{\Pi_{comp}}\left(N_{tc}, D_{comp}\right)$ and $\eta_{comp} = \mathrm{LUT}_{\eta_{comp}}\left(N_{tc}, D_{comp}\right)$ are mapped.

Similarly, the power delivered by the turbine can be written:

$$\mathbb{P}_{turb} = D_{turb}C_pT_{exh}\eta_{turb}\left(1 - \Pi_{turb}^{\frac{1-\gamma}{\gamma}}\right) \tag{8}$$

where the quantities $\eta_{turb} = \mathrm{LUT}_{\eta_{turb}}\left(N_{tc}, \Pi_{turb}\right)$ and $D_{turb} = \mathrm{LUT}_{D_{turb}}\left(N_{tc}, \Pi_{turb}\right)$ are mapped.

Note that the turbocharger variables (air flow and speed) are corrected to consider the variations of the thermodynamic conditions in the upstream (resp. downstream) of the compressor (resp. turbine) [10].

2.5. Complete Model for Control Design

By grouping equations (1), (2) and (6), the following dynamical system is obtained:

$$\begin{cases} \dfrac{dP_{man}}{dt} = K_{man}\left(D_{thr} - D_{cyl}\right) \\ \dfrac{dP_{exh}}{dt} = K_{exh}\left(K_{fuel}D_{cyl} - D_{turb} - D_{wg}\right) \\ \dfrac{d}{dt}\left(\dfrac{1}{2}J_{tc}N_{tc}^2\right) = \mathbb{P}_{turb} - \mathbb{P}_{comp} \end{cases} \tag{9}$$

The model (9) accurately describes the three main dynamics governing the turbocharged air system of a SI engine. This model will be directly used to design the nonlinear MIMO controller in Section 4.

3. Nonlinear Control System Design

Hereafter, only some bases on input-output linearization for control-affine MIMO nonlinear systems will be reminded, please refer to [11] for more details.

3.1. Input-Output Linearization for MIMO system

Consider the following MIMO nonlinear system:

$$\begin{cases} \dot{x} = f(x) + \sum_{i=1}^{m} g_i(x) u_i \\ y = h(x) \triangleq \left[h_1(x), \ldots, h_m(x) \right]^T \end{cases} \quad (10)$$

where $x \in \mathbb{R}^n$, $u \in \mathbb{R}^m$ and $y \in \mathbb{R}^m$ are respectively the system state, control input, and output vectors. The vector functions $f(x)$, $g(x)$ and $h(x)$ are assumed to be sufficiently smooth in a domain $D \subset \mathbb{R}^n$. The feedback linearization law of the system (10) is given as:

$$\begin{aligned} u &= \begin{bmatrix} L_{g_1} L_f^{\rho_1 - 1} h_1(x) & \ldots & L_{g_m} L_f^{\rho_1 - 1} h_1(x) \\ \ldots & \ldots & \ldots \\ L_{g_1} L_f^{\rho_m - 1} h_m(x) & \ldots & L_{g_m} L_f^{\rho_m - 1} h_m(x) \end{bmatrix}^{-1} \left(\begin{bmatrix} v_1 \\ \vdots \\ v_m \end{bmatrix} - \begin{bmatrix} L_f^{\rho_1} h_1(x) \\ \vdots \\ L_f^{\rho_m} h_m(x) \end{bmatrix} \right) \\ &\triangleq J^{-1}(x)\left(v - l(x)\right) \end{aligned} \quad (11)$$

where $\left[\rho_1 \ldots \rho_m\right]^T$ is the relative degree vector; $L_f^{\rho_i} h_i(x)$ and $L_{g_i} L_f^{\rho_i - 1} h_i(x)$ are the Lie derivatives of the scalar functions $h_i(x)$, $i = 1, \ldots, m$. Note that the control law (11) is well defined in the domain $D \subset \mathbb{R}^n$ if the *decoupling matrix* $J(x)$ is non-singular at every point $x_0 \in D \subset \mathbb{R}^n$. The new manipulated input vector v can be designed with any linear control technique. The relative degree of the system (10) in this case is defined as:

$$\rho = \sum_{k=1}^{m} \rho_k \quad (12)$$

3.2. Normal Form and Internal Dynamics Analysis

The system relative degree ρ plays an important role in feedback linearization control technique. Indeed, according to its value, three following cases are considered.

- ***Case 1:*** If $\rho = n$, then the nonlinear system (10) is fully feedback linearizable.
- ***Case 2:*** If $\rho < n$, then the nonlinear system (10) is partially feedback linearizable. In this case, there are some internal dynamics of order $(n - \rho)$. In tracking control, it should be guaranteed that these dynamics are well behaved, i.e. stable or bounded in some sense.
- ***Case 3:*** If ρ does not exist on the domain D, then the input-output linearization technique is not directly applicable with this technique.

The linearized system for the two first cases can be represented under the following *normal form* [11]:

$$\begin{cases} \dot{\xi} = A\xi + Bv \\ y = C\xi \\ \dot{\omega} = f_0(\omega, \xi, v) \end{cases} \quad (13)$$

where ξ and ω are respectively ρ-dimensional and $(n - \rho)$-dimensional state vector which are obtained with a suitable change of coordinates $z \triangleq T(x) \triangleq \left[\xi, \omega\right]^T$; the triplet (A, B, C) is in Brunovsky block canonical form; the last equation in (13) characterizes the internal dynamics [11]. It is worth noting that if the system $\dot{\omega} = f_0(\omega, \xi, v)$ is input-to-state stable, then the origin of system (13) is globally asymptotically stable [12] if v is a stabilizing control law for the first subsystem.

4. Application: Control of the Air System of a Turbocharged SI Engine

In this section, a MIMO nonlinear controller is designed for the air system presented in Section 2.

It is first very important to highlight the following fact. For almost all controllers existing in actual literature, not only available measures of engine intake side (i.e. P_{man}, T_{man}, P_{boost}, N_e) but also several other signals coming from the exhaust side are needed for controller implementation. These latter signals, i.e. P_{exh}, T_{exh}, P_{dt}, N_{tc} are not measured in series production vehicles and usually assumed to be given by some observers. To get rid of this assumption, in this work, these variables will be estimated by their static LUTs issued from the data measured in steady-state conditions in the test bench. As a consequence, the number of sensors or/and complex observers/estimators could be limited. Concretely, the following LUTs will be constructed:

$$\begin{cases} P_{exh} = \mathrm{LUT}_{P_{exh}}(N_e, P_{man}); \quad T_{exh} = \mathrm{LUT}_{T_{exh}}(N_e, D_{cyl}) \\ P_{dt} = \mathrm{LUT}_{P_{dt}}(N_e, D_{cyl}); \quad N_{tc} = \mathrm{LUT}_{N_{tc}}(\Pi_{comp}, D_{comp}) \end{cases} \quad (14)$$

It is worth noting from (14) that all the inputs of these LUTs P_{exh}, T_{exh}, P_{dt}, N_{tc} can be measured/computed with available sensors. In fact, the estimations in (14) are reasonable since SI engines operate at stoichiometric conditions which implies that all exhaust variables are highly correlated to the in-cylinder air mass flow (or intake manifold pressure) [9].

4.1. MIMO Controller Design

For control design purpose, besides the output of interest $y_{man} \triangleq P_{man}$, a second virtual one is introduced $y_{exh} \triangleq P_{exh}$. Note that, by means of LUT in (14), we can impose that $P_{exh,ref} = \mathrm{LUT}_{P_{exh}}(N_e, P_{man,ref})$ and, then, if P_{exh} converges to $P_{exh,ref}$, it implicitly makes P_{man} converge to $P_{man,ref}$. As a consequent, both outputs P_{man} and P_{exh} are used to control the intake pressure. Now, let us first consider the two pressure dynamics in (9) which are rewritten as:

$$\begin{cases} \dot{P}_{man} = K_{man}(D_{thr} - D_{cyl}) \triangleq f_{thr} + g_{thr} u_{thr} \\ \dot{P}_{exh} = K_{exh}(K_{fuel} D_{cyl} - D_{turb} - D_{wg}) \triangleq f_{wg} + g_{wg} u_{wg} \\ y_{man} \triangleq P_{man} \\ y_{exh} \triangleq P_{exh} \end{cases} \quad (15)$$

where

$$\begin{cases} K_{man} \triangleq \dfrac{RT_{man}}{V_{man}}; \quad g_{thr} \triangleq K_{man} \dfrac{P_{boost}}{\sqrt{RT_{man}}} \Phi\left(\Pi_{thr}^{*}\right); \\ K_{cyl} \triangleq \eta_{vol} \dfrac{V_{cyl}}{V_{man}} \dfrac{N_e}{30} P_{man}; \quad f_{thr} \triangleq -K_{man} D_{cyl}; \\ K_{fuel} \triangleq \left(1+\dfrac{1}{\lambda_s}\right); \quad g_{wg} \triangleq -K_{exh} \dfrac{P_{exh}}{\sqrt{RT_{exh}}} \Phi\left(\Pi_{wg}^{*}\right); \\ K_{exh} \triangleq \dfrac{RT_{exh}}{V_{exh}}; \quad f_{wg} \triangleq K_{exh}\left(K_{fuel} D_{cyl} - D_{turb}\right). \end{cases} \tag{16}$$

The time derivatives of the outputs of system (15) are given:

$$\begin{cases} \dot{y}_{man} = \dot{P}_{man} = f_{thr} + g_{thr} u_{thr} = v_{man} \\ \dot{y}_{exh} = \dot{P}_{exh} = f_{wg} + g_{wg} u_{wg} = v_{exh} \end{cases} \tag{17}$$

Remark that the two control inputs u_{thr}, u_{wg} appear respectively in $\dot{y}_{man}$, $\dot{y}_{exh}$; the signals v_{man} and v_{exh} are two new manipulated inputs. By using integral structure for tracking control purpose, the linearized system

$$\begin{cases} \dot{y}_{man} = v_{man} \\ \dot{y}_{exh} = v_{exh} \\ \dot{x}_{\text{int}} = y_{man,ref} - y_{man} \end{cases} \tag{18}$$

is straightforwardly derived from the system (15) with the following feedback linearization control laws:

$$\begin{cases} u_{thr} = -\dfrac{f_{thr}}{g_{thr}} + \dfrac{1}{g_{thr}} v_{man} \\ u_{wg} = -\dfrac{f_{wg}}{g_{wg}} + \dfrac{1}{g_{wg}} v_{exh} \end{cases} \tag{19}$$

Let us define $x \triangleq \left[y_{man}, y_{exh}, x_{\text{int}}\right]^T$ and $v \triangleq \left[v_{man}, v_{exh}\right]^T$. Then, the linearized system (18) is rewritten as:

$$\dot{x} = \begin{pmatrix} 0 & 0 & 0 \\ 0 & 0 & 0 \\ -1 & 0 & 0 \end{pmatrix} x + \begin{pmatrix} 1 & 0 \\ 0 & 1 \\ 0 & 0 \end{pmatrix} v + \begin{pmatrix} 0 \\ 0 \\ 1 \end{pmatrix} y_{man,ref} \tag{20}$$

In this work, the state feedback law $v = -K\xi$ is designed through a simple pole-placement approach. The following control gain will be implemented in the simulator:

$$v = -Kx = -\begin{bmatrix} 140 & 0 & -2400 \\ 0 & 50 & 0 \end{bmatrix} x \tag{21}$$

Note that the tracking problem has been solved accounting only for a part of the closed-loop system (9). The stability analysis of the following internal dynamics N_{tc}^2 is necessary:

$$\frac{d}{dt}\left(N_{tc}^2\right) = K_{turb} D_{turb} - K_{comp} D_{comp} \tag{22}$$

where

$$\begin{cases} K_{turb} \triangleq \dfrac{2}{J_{tc}} C_p T_{exh} \eta_{turb} \left(1 - \Pi_{turb}^{\frac{1-\gamma}{\gamma}}\right) \\ K_{comp} \triangleq \dfrac{2}{J_{tc}} C_p T_{amb} \dfrac{1}{\eta_{comp}} \left(\Pi_{comp}^{\frac{\gamma-1}{\gamma}} - 1\right) \end{cases} \tag{23}$$

Furthermore, from (15) and (17), one gets:

$$D_{turb} = K_{fuel} D_{cyl} - D_{wg} - \frac{v_{exh}}{K_{exh}} \tag{24}$$

It follows from (22) and (24) that:

$$\frac{d}{dt}\left(N_{tc}^2\right) = -K_{turb} D_{wg} - K_{comp} D_{comp} + K_{turb} K_{fuel} D_{cyl} - \frac{K_{turb}}{K_{exh}} v_{exh} \tag{25}$$

Note that $P \triangleq \left[P_{man}, P_{exh}\right]^T$ can be seen as the input vector of system (25) and it follows from (21) that:

$$\begin{aligned} \dot{N}_{tc}^2 &< \sqrt{\left(K_{turb} K_{fuel} K_{cyl}\right)^2 + \left(\frac{K_{turb}}{K_{exh}} K_{(2,2)}\right)^2} \left\|P\right\| - K_{comp} D_{comp} \\ &\triangleq \alpha(\cdot)\left\|P\right\| - \beta\left(N_{tc}^2\right) \end{aligned} \tag{26}$$

Since $\alpha(\cdot)$ is bounded and the function $\beta(\cdot)$ is of class $\mathcal{K}^{\infty}$ (its curve form is not depicted here due to lack of space). Then, it can be deduced that the system (22) is always input-to-state stable [13].

4.2. Fuel-Optimal Control Strategy

Until now, we have designed in this work a so-called *Conventional MIMO controller* with two inputs: throttle, wastegate and two outputs: intake pressure, exhaust pressure. However, this controller is not *optimal* in the sense of energy losses minimization. Indeed, it is known that the wastegate should be opened as much as possible at a given operating point to minimize the pumping losses [1]. This concept generally leads to the following strategy: in low load zone, only the throttle is used to track the intake pressure, the wastegate is widely open and in high load zone, the wastegate is activated to control the pressure while the throttle is widely open. Although this strategy offers many advantages concerning the fuel economy benefits and also the control design simplification (only one actuator is controlled at a time), it may overcharge the wastegate in some cases since the torque response is slower for this actuator than for the throttle. To overcome this eventual difficulty while taking fully into account the fuel-optimal strategy, we propose here a so-called *Fuel-optimal controller*. This novel controller is directly derived from the *Conventional MIMO controller* and they both have the same auxiliary control law given in (21).
It can be deduced from the second equation of (15) that:

$$D_{cyl} = \frac{v_{exh}}{K_{exh} K_{fuel}} + \frac{D_{turb}}{K_{fuel}} + \frac{D_{wg}}{K_{fuel}} \tag{27}$$

With this new expression of the in-cylinder mass air flow, the intake pressure dynamics can be also rewritten as:

$$\dot{P}_{man} = K_{man}\left(D_{thr} - \frac{v_{exh}}{K_{exh} K_{fuel}} - \frac{D_{turb}}{K_{fuel}} - \frac{D_{wg}}{K_{fuel}}\right) = v_{man}$$

or

$$\dot{P}_{man} = g_{thr} u_{thr} - \frac{K_{man}}{K_{exh} K_{fuel}} v_{exh} - \frac{K_{man}}{K_{fuel}} D_{turb} + \frac{K_{man}}{K_{exh} K_{fuel}} g_{wg} u_{wg} \tag{28}$$

The novel *Fuel-optimal controller* is directly derived from expression (28). To this end, the engine operating range is divided into three zones according to two predefined intake pressure thresholds $P_{man,1}$ and $P_{man,2}$. Each operating zone has its own actuator scheduling strategy as described below:

- ***Zone 1*** (low load zone $P_{man} \le P_{man,1}$): The wastegate is widely open and the throttle is solely used to track the intake pressure reference. Let $S_{wg,\max}$ be the maximal opening

section of the wastegate. The implemented actuator control laws are in this case:

$$\begin{cases} u_{thr} = \dfrac{1}{g_{thr}}\left(\dfrac{K_{man}}{K_{exh}K_{fuel}}v_{exh} + \dfrac{K_{man}}{K_{fuel}}D_{turb} - \dfrac{K_{man}}{K_{exh}K_{fuel}}g_{wg}S_{wg,\max} + v_{man}\right) \\ u_{wg} = S_{wg,\max} \end{cases} \quad (29)$$

- ***Zone 2*** (middle load zone $P_{man,1} < P_{man} < P_{man,2}$): Both throttle and wastegate are simultaneously used to control the intake pressure. In this case, the implemented actuator control laws are exactly the feedback linearization laws in (19), which are recalled here:

$$u_{thr} = -\frac{f_{thr}}{g_{thr}} + \frac{1}{g_{thr}}v_{man}; \qquad u_{wg} = -\frac{f_{wg}}{g_{wg}} + \frac{1}{g_{wg}}v_{exh} \quad (30)$$

- ***Zone 3*** (high load zone $P_{man} \geq P_{man,2}$): The throttle is fully opened and only the wastegate is activated to control the intake pressure which is approximated by the boost pressure P_{boost}. The implemented actuator control laws are:

$$\begin{cases} u_{thr} = S_{thr,\max} \\ u_{wg} = \dfrac{K_{exh}K_{fuel}}{K_{man}g_{thr}}\left(\dfrac{K_{man}}{K_{exh}K_{fuel}}v_{exh} + \dfrac{K_{man}}{K_{fuel}}D_{turb} - g_{thr}S_{thr,\max} + v_{man}\right) \end{cases} \quad (31)$$

where $S_{thr,\max}$ is the maximal opening section of the throttle.

Several remarks can be made for this actuator scheduling strategy. First, the new input vector v is kept to be the same for all three zones. Second, when the wastegate (resp. throttle) is saturated in Zone 1 (resp. Zone 3), the exhaust (resp. intake) pressure dynamics is input-to-state stable with respect to the intake (resp. exhaust) pressure (the proof is omitted due to lack of space). Third, it can be concluded from the above remarks that if the intake pressure tracking is guaranteed, then all other variables of the air system will be well behaved in spite of the fact that the engine operating range is divided into three zones. Fourth, the model-based *Fuel-optimal controller* is based on a "dummy" switching strategy because no switching model has been used in this approach. Fifth, the pressure threshold values $P_{man,1}$ and $P_{man,2}$ separating the three zones are "freely" chosen thanks to the propriety of the above fourth remark. However, they are usually very close for engine efficiency benefits.

It is worth noting that *Fuel-optimal controller* is different from other existing nonlinear approaches in the literature. As the approach proposed in [5], this novel controller is a MIMO nonlinear controller which can guarantee the closed-loop stability of the whole turbocharged engine air system. However, the novel *Fuel-optimal controller* is much simpler and the middle-load zone (Zone 2) is very easily introduced to improve the torque response at high load while maintaining the maximum possible the advantage of *fuel-optimal* concept in [1]. Compared with the approach in [4] which is also based on feedback linearization, our approach does not need any model simplification, e.g. neglecting pressure dynamics with respect to turbocharger dynamics according to singular perturbation theory and then approximating the turbocharger square speed as a linear function of compressor pressure ratio. Moreover, in [4], the authors only proposed the control for the wastegate and this approach cannot take into account the mid-load zone.

5. Simulation Results and Analysis

Hereafter, a series of trials are performed on an advanced engine simulator designed under commercial AMESim platform to show the effectiveness of the proposed approach for both cases: *Conventional MIMO controller* and *Fuel-optimal controller*. For the sake of clarity, the two commands (throttle, wastegate) are normalized. The control inputs constraints become: $0 \leq \bar{u}_{thr}, \bar{u}_{wg} \leq 100\%$. When $\bar{u}_{thr} = 100\%$ (resp. $\bar{u}_{wg} = 0\%$), it means that the throttle (resp. wastegate) is fully open. On the reverse, when $\bar{u}_{thr} = 0\%$ (resp. $\bar{u}_{wg} = 100\%$), the throttle (resp. wastegate) is fully closed. In the following simulations at $N_e = 2000$ rpm, the pressure thresholds are chosen as $P_{man,1} = 0.9$ bar and $P_{man,2} = 1.2$ bar.

Figure 2 and Figure 3 respectively represent the tracking performance and the corresponding actuator responses for *Conventional MIMO controller* and *Fuel-optimal controller*. Several comments can be reported as follows. First, *Conventional MIMO controller* simultaneously uses both actuators to track the intake pressure while these actuators are "optimally" scheduled by the strategy described in Subsection 4.2 with *Fuel-optimal controller*. Second, the wastegate is opened very little with *Conventional MIMO controller* so that the boost potential of the turbocharger can be fully exploited. Hence, the closed-loop time response with this controller is faster than the one of *Fuel-optimal controller* in middle and high load zones. Third, although *Conventional MIMO controller* can be used to improve the torque response (drivability), this controller is not optimal in terms of fuel consumption compared with *Fuel-optimal controller* as shown in Figure 4. The pumping losses with *Fuel-optimal controller* are almost lower than the ones with *Conventional MIMO controller* at every time.

Figure 5 shows the comparison, in the case of *Fuel-optimal controller*, between the exhaust pressure given by the simulator AMESim and its static LUT which is used to compute the controller. Note that although some higher dynamics are missing and there are some slight static errors, the tracking performance of both controllers is very satisfying.

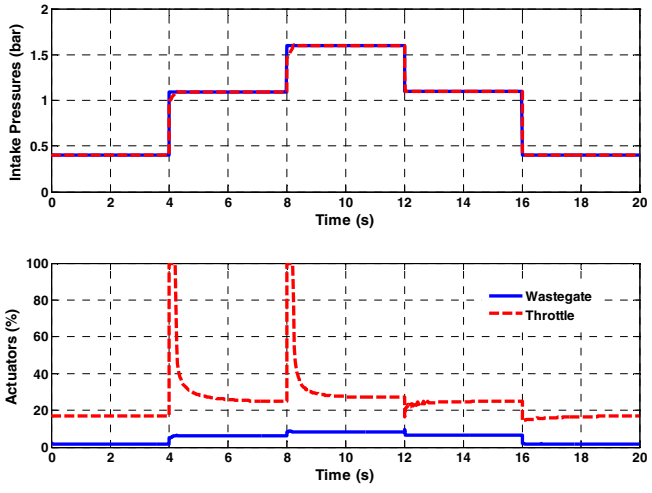

Figure 2. Pressure tracking performance and corresponding actuator responses with *Conventional MIMO controller*

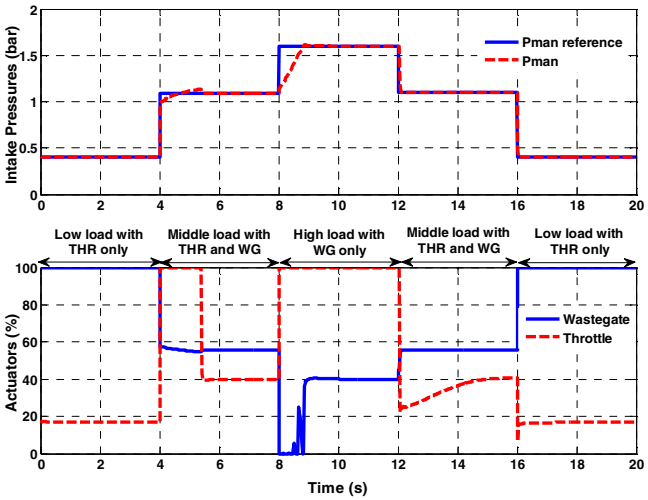

Figure 3. Pressure tracking performance and corresponding actuator responses with *Fuel-optimal controller*

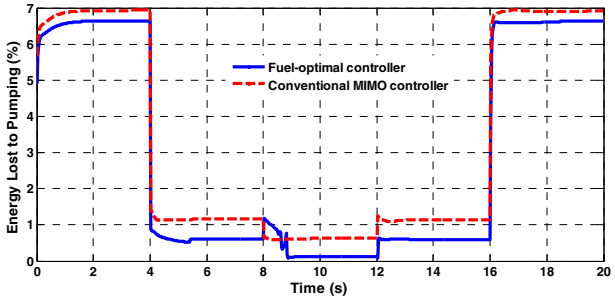

Figure 4. Comparison of engine pumping losses between *Conventional MIMO controller* and *Fuel-optimal controller*

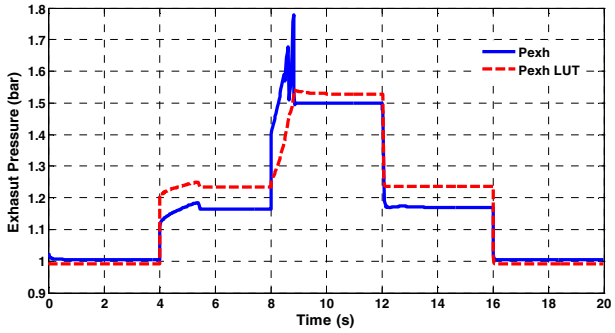

Figure 5. Comparison between the exhaust pressure given by the simulator AMESim and its static LUT model

6. Conclusions

In this paper, a novel approach has been proposed to control the turbocharged air system of a SI engine. Several advantages of this approach can be summarized as follows. First, the second virtual output $y_{exh} \triangleq P_{exh}$ is introduced by means of LUT and this fact drastically simplifies the control design task. Second, the resulting nonlinear control law is very easily implementable. Third, offline engine data of the test bench is effectively reused and exploited for engine control development so that the number of sensors and/or observers/estimators could be limited. Despite its simplicity, the proposed approach performs very promising results for both control strategies, i.e. to improve the drivability with *Conventional MIMO controller* or to optimize the fuel consumption with *Fuel-optimal controller*.

Handling the model uncertainties is known as one of major drawbacks of feedback linearization based controllers. The study on robust design will be investigated in future research.

Acknowledgments

This research was supported by the International Campus on Safety and Intermodality in Transportation, the Nord-Pas-de-Calais Region, the European Community, the Regional Delegation for Research an Technology, the Ministry of Higher Education and Research, and the French National Center for Scientific Research. The authors gratefully acknowledge the VALEO Company for their supports in the framework of the SURAL-HY project. We would also like to thank Prof. Marie-Thierry Guerra, Director of LAMIH for his valuable supports in the collaboration framework with Prof. Michio Sugeno, Emeritus Researcher from European Centre for Soft Computing, Spain.

References

[1] L. Eriksson, S. Frei, C. Onder, and L. Guzzella, "Control and Optimization of Turbocharged SI Engines," in *15th IFAC World Congress*, Barcelona, Spain, 2002.

[2] A. Karnik, J. Buckland, and J. Freudenberg, "Electronic Throttle and Wastegate Control for Turbocharged Gasoline Engines," in *American Control Conference*, Portland, 2005, pp. 4434-4439.

[3] L. Daubler, C. Bessai, and O. Predelli, "Tuning Strategies for Online-Adaptive PI Controller," *Oil & Gas Science and Technology - Rev. IFP*, vol. 62, no. 4, pp. 493-500, 2007.

[4] P. Moulin and J. Chauvin, "Modeling and Control of the Air System of a Turbocharged Gasoline Engine," *Control Engineering Practice*, vol. 19, no. 3, pp. 287-297, 2011.

[5] A.T. Nguyen, J. Lauber, and M. Dambrine, "Robust H_∞ Control Design for Switching Uncertain System: Application for Turbocharged Gasoline Air System Control," in *51st Conference on Decision and Control*, Maui, Hawaii, USA, 2012, pp. 4265-4270.

[6] T. Takagi and M. Sugeno, "Fuzzy Identification of Systems and Its Applications to Modeling and Control," *Trans. on Systems, Man and Cybernetics*, vol. 15, no. 1, pp. 116-132, 1985.

[7] AT. Nguyen, J. Lauber, and M. Dambrine, "Switching Fuzzy Control of the Air System of a Turbocharged SI Engine," in *IEEE International Conference on Fuzzy Systems*, Brisbane, Australia, 2012, pp. 893-899.

[8] L. Guzzella and C. Onder, *Introduction to Modeling and Control of Internal Combustion Engine Systems*. Springer, 2004.

[9] L. Eriksson, "Modeling and Control of Turbocharged SI and DI Engines," *Oil & Gas Science and Technologies*, vol. 62, no. 4, pp. 523-538, 2007.

[10] P. Moraal and I. Kolmanovsky, "Turbocharger Modeling for Automotive Control Applications," *SAE Technical Paper Series*, vol. no. 1999-01-0908, 1999.

[11] A. Isidori, *Nonlinear Control Systems*. Springer Verlag, 1989.

[12] H.K. Khalil, *Nonlinear Systems*, 3rd ed.: Prentice Hall, 2002.

[13] E. Sontag and Y. Wang, "On Characterizations of the Input to State Stability Property," *Systems and Control Letters*, vol. 24, pp. 351-359, 1995.